

FUSE Observations of O VI Absorption in the Galactic Halo

B.D. Savage¹, K.R. Sembach², E.B. Jenkins³, J.M. Shull⁴, D.G. York⁵, G. Sonneborn⁶, H.W. Moos², S.D. Friedman², J.C. Green⁴, W.R. Oegerle², W.P. Blair², J.W. Kruk², E.M. Murphy²

ABSTRACT

Far-ultraviolet spectra of 11 AGNs observed by FUSE are analyzed to obtain measures of O VI $\lambda 1031.93$ absorption occurring over very long paths through Milky Way halo gas. Strong O VI absorption is detected along 10 of 11 sight lines. Values of $\log[N(\text{O VI}) \sin |b|]$ range from 13.80 to 14.64 with a median value of 14.21. The observations reveal the existence of a widespread but irregular distribution of O VI in the Milky Way halo. Combined with estimates of the O VI mid-plane density, $n_0 = 2 \times 10^{-8} \text{ cm}^{-3}$, from the *Copernicus* satellite, the FUSE observations imply an O VI exponential scale height of 2.7 ± 0.4 kpc. We find that $N(\text{C IV})/N(\text{O VI})$ ranges from ~ 0.15 in the disk to ~ 0.6 along four extragalactic sight lines. The changing ionization state of the gas from the disk to the halo is consistent with a systematic decrease in the scale heights of Si IV, C IV, N V, to O VI from ~ 5.1 to ~ 2.7 kpc. While conductive heating models can account for the highly ionized atoms at low $|z|$, a combination of models (and processes) appears to be required to explain the highly ionized atoms found in the halo. The greater scale heights of Si IV and C IV compared to O VI suggests that some of the Si IV and C IV in the halo is produced in turbulent mixing layers or by photoionization by hot halo stars or the extragalactic background.

Subject headings: Galaxy: halo – Galaxy: structure – ISM: atoms – ISM: structure – ultraviolet: ISM

1. Introduction

In the fundamental paper “On a Possible Interstellar Galactic Corona,” Spitzer (1956) discussed the physical basis for the possible existence of a hot interstellar gas phase extending away from the Galactic plane into the halo. He also noted the diagnostic potential of the resonance doublet absorption lines of the Li-like ions of O VI, N V, and C IV for studying the coronal Galactic halo gas. Under conditions of equilibrium collisional ionization, these three ions peak in abundance at $(3, 2, 1) \times 10^5$ K, respectively (Sutherland & Dopita 1993).

Interstellar O VI observations were obtained by Jenkins (1978a, b) and York (1977) using the high resolution far-UV spectrometer aboard the *Copernicus* satellite. Those observations provided fundamental information about the hot interstellar gas in the disk of the Milky Way but were limited to stars brighter

¹Department of Astronomy, University of Wisconsin, Madison, WI 53706

²Department of Physics & Astronomy, The Johns Hopkins University, Baltimore, MD 21218

³Princeton University observatory, Princeton, NJ 08544

⁴CASA and JILA, Department of Astrophysical & Planetary Sciences, University of Colorado, Boulder, CO 80309

⁵Astronomy & Astrophysics Dept., University of Chicago, Chicago 60637

⁶NASA/GSFC, Greenbelt, MD 20771

than $V \sim 7.0$. The *International Ultraviolet Explorer* (IUE) and the *Hubble Space Telescope* (HST) allowed astronomers to study absorption by N V, C IV, and Si IV in the Galactic halo (Savage & de Boer 1979; Savage & Massa 1987; Sembach & Savage 1992; Savage, Sembach, & Lu 1997), but O VI was unobservable because windowless detectors and specially coated optics are required to measure the O VI $\lambda\lambda 1031.93, 1037.62$ doublet. O VI has a special significance among the high ionization species because it is a sensitive indicator of collisionally ionized gas and is the least likely to be produced by photoionization from starlight given that 113.9 eV are required for the conversion of O V to O VI.

Except for brief observing programs by the *Hopkins Ultraviolet Telescope* (HUT; Davidsen 1993), and the spectrographs in the *Orbiting and Retrievable Far and Extreme Ultraviolet Spectrometers* (ORFEUS; Hurwitz & Bowyer 1996; Hurwitz et al. 1998; Widmann et al. 1999; Sembach, Savage, & Hurwitz 1999), we have had a long hiatus in observing O VI. This has ended with the commissioning of the *Far-Ultraviolet Spectroscopic Explorer* (FUSE), a facility that has been specially designed to cover wavelengths from 905 to 1187 Å with an efficient 2-dimensional detector. The spectroscopic capabilities of FUSE and its in-flight performance are discussed by Moos et al. (2000) and Sahnou et al. (2000). This paper reports on initial FUSE results for O VI absorption in the Galactic halo.

2. FUSE Observations and Data Processing

The spectral integrations with FUSE were obtained in the time-tagged photon address mode between September and December 1999. The observations were obtained with the objects centered in the large $30'' \times 30''$ aperture of the LiF1 channel and generally extended over spacecraft night and day. Most of the effective area in the O VI $\lambda\lambda 1031.93, 1037.62$ wavelength region is provided by the spectra obtained with the LiF channels. We have restricted our analysis to the observations in the LiF1 channel.

To produce the final composite spectra in the region of O VI, we followed the basic data handling procedures discussed by Sembach et al. (2000). The spectra have a velocity resolution of approximately 25 km s^{-1} (FWHM). The zero point of the wavelength scale in the vicinity of the O VI lines was determined with reference to nearby H₂ lines or Si II and O I lines. Sample FUSE spectra extending from 1020 to 1045 Å for Ton S210 and PG 0804+761 are shown in Figure 1.

3. Interstellar Analysis

The weaker O VI $\lambda 1037.62$ line is near strong absorption by C II* $\lambda 1037.02$ and the H₂ (5–0) R(1) and P(1) lines at 1037.15 and 1038.16 Å. The stronger O VI $\lambda 1031.93$ line is usually relatively free of blending with other species since the nearby H₂ (6–0) R(3) and R(4) lines at 1031.19 and 1032.36 Å are often weak and well-separated in velocity from O VI ($\Delta v = -214$ and $+125 \text{ km s}^{-1}$, respectively). Blending from the HD (6–0) R(0) and R(1) lines at 1031.93 and 1032.36 Å is not a problem because the amount of molecular gas along these sight lines is small (Shull et al. 2000). For most paths through the Galactic halo, the contamination of the O VI $\lambda 1037.62$ line is severe. Therefore, we concentrate our attention on the O VI $\lambda 1031.93$ line in this Letter and use the $\lambda 1037.62$ line only to evaluate possible saturation in the $\lambda 1031.93$ absorption.

The O VI $\lambda 1031.93$ absorption is sufficiently broad that it is nearly fully resolved by FUSE. Therefore, we converted the observed absorption line profiles into measures of O VI apparent column density per unit

velocity, $N_a(v)$, through the relation $N_a(v)$ [ions cm^{-2} $(\text{km s}^{-1})^{-1}$] = $m_e c / \pi e^2 \tau_a(v) (f\lambda)^{-1} = 3.768 \times 10^{14} \tau_a(v) (f\lambda)^{-1}$, where $f=0.133$ is the oscillator strength of the $\lambda 1031.93$ line (Morton 1991), λ is the wavelength in \AA , and $\tau_a(v)$ is the apparent absorption optical depth (see Savage & Sembach 1991). The continuum levels are well-defined by the smooth flux distributions provided by the AGNs. For cases where the O VI $\lambda 1037.62$ line could be measured, we find the same values of $\log N_a(v)$ near maximum absorption as those obtained for the stronger $\lambda 1031.93$ line. Therefore, there is no evidence for unresolved saturated structure in the O VI absorption.

Values of the integrated apparent O VI column density are given in Table 1 along with errors including statistical and continuum placement uncertainties (Sembach & Savage 1992). Column densities and equivalent widths were integrated over the velocity range spanned by v_- to v_+ as listed in Table 1.

4. O VI Profiles

The O VI absorption profiles illustrated in Figure 1 and in Sembach et al. (2000) are often complex and trace a wide range of phenomena in or near the Milky Way. Those portions of the profiles between approximately -100 and $+100 \text{ km s}^{-1}$ are likely tracing gas in the thick O VI halo of the Milky Way, which is the primary subject of this paper. However, an inspection of the O VI profiles reveals high velocity ($100 < |v| < 300 \text{ km s}^{-1}$) O VI absorption toward 7 of the 12 objects: Mrk 876, Mrk 509, PKS 2155-304, H 1821+643, NGC 7469, Ton S180, and Ton S210. Sembach et al. (2000) discuss the properties and possible origins of this high velocity O VI absorption. We comment on one case here. The O VI absorption toward H 1821+653 reveals local gas at $v = 0$, gas above the Perseus spiral arm at $v = -70 \text{ km s}^{-1}$, and gas in the outer warped region of the outer Milky Way at $v = -120 \text{ km s}^{-1}$ (Oegerle et al. 2000). In calculating the column densities listed in Table 1, the velocity limits were set to exclude high velocity O VI except for H 1821+643, where the value of $N(\text{O VI})$ includes the outer Galaxy gas absorption extending to $v = -160 \text{ km s}^{-1}$. This high velocity O VI absorption is likely produced by differential Galactic rotation, which causes the absorption to extend to large negative velocities.

5. The Distribution of O VI in the Halo

Total column densities of O VI through the Galactic halo coupled with estimates of the mid-plane space density of O VI, n_0 , can be used to obtain information about the stratification of O VI away from the plane of the Galaxy. We assume an exponential gas stratification with $n(|z|) = n_0 \exp(-|z|/h)$, where h is the O VI scale height. It then follows that the O VI column density perpendicular to the plane for an object with latitude b is given by $N(\text{O VI}) \sin |b| = n_0 h [1 - \exp(-|z|/h)]$, where $N(\text{O VI})$ is the line-of-sight column density to an object at a distance $|z|$ away from the plane. For extragalactic objects, where $|z| \gg h$, $N(\text{O VI}) \sin |b| = n_0 h$.

Values of $\log[N(\text{O VI}) \sin |b|]$ toward 11 extragalactic objects observed by FUSE are listed in Table 1 along with the ORFEUS value for 3C 273 from Hurwitz et al. (1998). The large value (14.80) for the 3C 273 sight line is likely a consequence passing through Radio Loops I and IV and the North Polar Spur. Such structures are local examples of the regions that likely feed hot gas into the halo. Since the 3C 273 sight line is a special case, we do not include it in our synthesis of general conclusions below. Without 3C 273, the median $\log[N(\text{O VI}) \sin |b|]$ in our sample is 14.21 with a spread of 0.4 dex. The irregular nature of the distribution is highlighted by the low value of 13.80 found toward VII Zw118 which lies ~ 14 degrees from

PG 0804+761 and has $\log[N(\text{O VI})\sin |b|] = 14.21$. These irregularities must be considered when estimating the O VI scale height.

From the *Copernicus* observations of O VI absorption toward hot stars, Jenkins (1978b) estimated a mid-plane density $n_0 = 2.8 \times 10^{-8} \text{ cm}^{-3}$. However, that estimate assumed a small scale height (0.3 kpc) for the O VI absorbing layer, based on the limited data available at the time. We now find that the scale height must be about 10 times larger. Accordingly, we have obtained a new estimate of n_0 from the *Copernicus* O VI survey that is appropriate for a large scale height O VI absorbing layer with $h > 2$ kpc. The result is $n_0 = \Sigma N(\text{O VI}) / \Sigma r_0 = 2.0 \times 10^{-8} \text{ cm}^{-3}$, where the reduced distance $r_0 = h[1 - \exp(-|z|/h)]\text{csc } |b|$, compensates for the small reduction in density away from the Galactic plane. This value for n_0 was obtained when all of the upper limits for the *Copernicus* O VI column densities were included at their stated values. If zero is substituted for these cases, a value of n_0 that is only 5% lower is obtained. This value of n_0 has not been adjusted to allow for the fact that we live in the Local Bubble. Shelton & Cox (1994) have reanalyzed the *Copernicus* O VI measurements and have estimated that the mid-plane O VI density beyond the Local Bubble is $n_0 = (1.3 - 1.5) \times 10^{-8} \text{ cm}^{-3}$ for an O VI absorbing layer with $h \sim 3$ kpc.

For an O VI mid-plane density of $2.0 \times 10^{-8} \text{ cm}^{-3}$, we obtain the scale heights listed in Table 1 from the simple relation $h = N(\text{O VI})\sin |b|/n_0$. Ignoring 3C 273, the values range from 1.0 to 7.0 kpc. We find median and average values of 2.6 and 2.9 kpc, respectively. In deriving this average and in the subsequent calculations we treat the upper limit for PG 0052+251 as a detection. If we adopt the Shelton & Cox (1994) mid-plane density estimate of $1.4 \times 10^{-8} \text{ cm}^{-3}$ and reduce the extragalactic column densities by $1.5 \times 10^{13} \text{ cm}^{-2}$ to remove the Local Bubble contribution, we obtain median and average O VI scale heights of 3.5 and 4.0 kpc. Our incomplete knowledge of the mid-plane density introduces a 35% systematic uncertainty in the derivation of the O VI scale height. Another source of uncertainty involves the irregular distribution of the gas. Edgar & Savage (1989) devised an analysis procedure for estimating scale heights that accounts for the irregular distribution. The analysis includes a logarithmic patchiness parameter, σ_p , that is added in quadrature to the observed logarithmic errors in the column densities. The value of σ_p is varied until the minimized reduced chi square, $\chi^2_\nu(\text{min})$, of the scale height fit is acceptable. Using $n_0 = 2.0 \times 10^{-8} \text{ cm}^{-3}$ and the 11 FUSE values of $N(\text{O VI}) \sin |b|$, we obtain $\chi^2_\nu(\text{min}) = 1.0$ for $h = 2.7$ kpc and $\sigma_p = 0.21$ dex. Adopting this value of σ_p , we can then estimate the 1σ error in the scale height by determining the values of h where $\chi^2 = \chi^2(\text{min}) + 1.0$. The final result is $h(\text{O VI}) = 2.7 \pm 0.4$ kpc, where the listed 1σ errors do not include the additional 35% systematic uncertainty caused by the uncertain O VI mid-plane density and Local Bubble correction.

The O VI scale height of 2.7 ± 0.4 kpc can be compared with the values of $h = 5.1 \pm 0.7$, 4.4 ± 0.6 , and 3.9 ± 1.4 kpc for Si IV, C IV, and N V, respectively, determined by Savage et al. (1997) from HST and IUE observations. The more confined distributions of O VI and N V compared to C IV are also apparent in plots of $N(\text{C IV})/N(\text{O VI})$ and $N(\text{C IV})/N(\text{N V})$ versus $|z|$ toward objects in the disk and halo of the Galaxy. In each case there is a clear increase in the ratio from the disk to the halo, suggesting that C IV is more extended than O VI and N V. For N V the ratio increases by about a factor of 2 from low to high $|z|$ (see Fig. 6d in Savage et al. 1997). Spitzer (1996) noted that the value of $N(\text{C IV})/N(\text{O VI})$ increases from ~ 0.15 in the disk to 0.9 for objects in the low halo with $|z| \sim 1.5$ kpc. Values of $N(\text{C IV})$ have been measured using HST for Mrk 509, PKS 2155-304, 3C 273, H 1821+643, and ESO 141-55 by Savage et al. (1997) and by Sembach et al. (1999). Combining these with the values of $N(\text{O VI})$ from Table 1, we obtain $N(\text{C IV})/N(\text{O VI}) = 0.58$, 0.63, 0.45, 0.63 and 1.74, respectively, for the five extragalactic objects. The increase in this ratio by about a factor of 4 from the disk to the typical extragalactic halo sight line implies a large change in the ionization state of the highly ionized gas as a function of distance from the Galactic plane.

A major goal of the FUSE O VI program is to map out the distribution of O VI in the disk and halo of the Galaxy. Once we obtain FUSE O VI observations for a substantial number of disk and halo stars and for additional extragalactic objects it will be possible to improve on our initial estimate of the extension of O VI into the Galactic halo. These future studies will allow us to determine if a plane parallel, exponentially stratified, and patchy layer is indeed the most appropriate description of the distribution of O VI.

6. The Origin of Highly Ionized Atoms in the Galactic Halo

Strong O VI absorption toward 10 of 11 extragalactic objects observed by FUSE implies the widespread existence of hot gas in the halo of the Milky Way as predicted by Spitzer (1956) and also supported by the earlier observations of C IV and N V with IUE and HST. The decreasing scale heights in the sequence Si IV, C IV, N V, to O VI provides information about the changing ionization state of the gas with distance from the Galactic plane. Differences from element to element in the destructive liberation of atoms from dust grains could also influence the relative behavior of the z distributions of the highly ionized atoms.

Reviews of the many theories for the origins of the highly ionized atoms in the ISM are found in Spitzer (1990,1996) and Sembach, Savage, & Tripp (1997). The three primary types of theories involve conductive heating (CH) where cool gas evaporates into an adjacent hot medium, radiative cooling (RC) where hot gas cools as it flows into the halo or down onto the disk, and turbulent mixing layers (TML) where hot and cool gas are mixed through turbulent entrainment (Slavin, Shull, & Begelman 1993). Table 2 of Spitzer (1996) provides a summary of the many models along with the references to the theoretical literature. The different models make specific predictions for the expected values of $N(\text{C IV})/N(\text{O VI})$. The CH models are compatible with the value of $N(\text{C IV})/N(\text{O VI}) \sim 0.15$ found at low $|z|$, while the larger values of ~ 0.6 found toward the extragalactic objects observed by FUSE are better explained by a combination of the RC and TML models.

Shull & Slavin (1994) developed a hybrid model for the highly ionized gas in the Galactic halo in order to explain the smaller scale height of N V compared to Si IV and C IV suggested by the IUE and HST observations available in 1994. In their model the highly ionized ions at low $|z|$ are produced mainly in isolated SNRs while those at high $|z|$ are mainly found in radiatively cooling superbubbles that break through the disk producing Rayleigh-Taylor instabilities and turbulent mixing layers. Possible support for the origin of the high ions at low $|z|$ in isolated SNRs follows from the detailed SNR modeling of Shelton (1998). Confirmation that the scale height difference (smaller scale heights for ions with higher ionization potentials) first seen for N V and C IV is also clearly present in the new FUSE O VI measurements suggests that such hybrid models offer substantial promise for explaining the origin of the highly ionized species in the Galactic halo. Another example of a hybrid model is that of Ito & Ikeuchi (1988) which includes the cooling gas of a Galactic fountain flow (Shapiro & Field 1976) to provide the hot collisionally ionized gas and photoionization from the extragalactic background (Hartquist, Pettini, & Tallant 1984; Fransson & Chevalier 1985) to assist in the production of Si IV and C IV. The ionizing photons might also be provided by hot white dwarfs (Dupree & Raymond 1983). The new observations with FUSE imply several processes may be required to achieve a more complete understanding of the origins of the low density highly ionized gas extending away from the Galactic plane.

This work is based on data obtained for the Guaranteed Time Team by the NASA-CNES-CSA FUSE mission operated by the Johns Hopkins University. Financial support to U. S. participants has been provided

by NASA contract NAS5-32985.

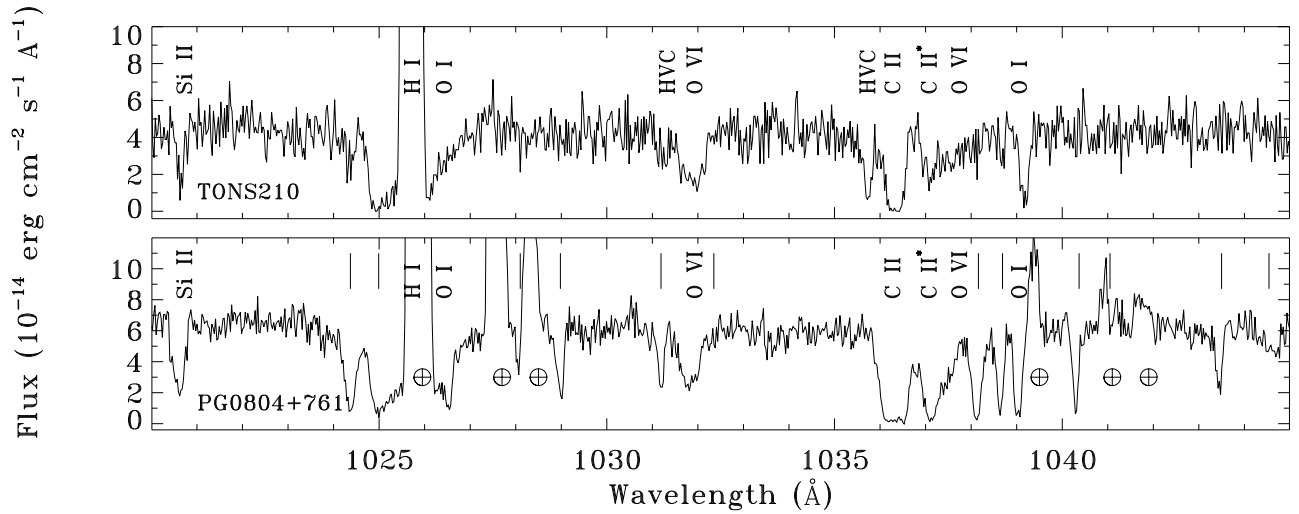
REFERENCES

- Davidson, A. F. 1993, *Science*, 259, 327
- Dupree, A. K., & Raymond, J. C. 1983, *ApJ*, 275, L71
- Edgar, R. J., & Savage, B. D. 1989, *ApJ*, 340, 762
- Fransson, C., & Chevalier, R. A. 1985, *ApJ*, 296, 35
- Hartquist, T. W., Pettini, M., & Tallant, A. 1984, 276, 519
- Hurwitz, M., & Bowyer, S. 1996, *ApJ*, 446, 812
- Hurwitz, M., et al. 1998, *ApJ*, 500, L61
- Ito, M., & Ikeuchi, S. 1988, *PASJ*, 40, 403
- Jenkins, E. B. 1978a, *ApJ*, 219, 845
- Jenkins, E.B. 1978b, *ApJ*, 220, 107
- Moos, H. W., et al 2000, *ApJ*, this issue
- Morton, D. C. 1991, *ApJS*, 77, 119
- Murphy, E. M., et al. 2000, *ApJ*, this issue
- Oegerle, W. R. et al. 2000, *ApJ*, this issue
- Savage, B. D., & de Boer, K.S. 1979, *ApJ*, 230, L77
- Savage, B. D., & Massa, D. 1987, *ApJ*, 314, 380
- Savage, B. D., Sembach, K.R., & Lu, L. 1997, *AJ*, 113, 2158
- Savage, B. D., & Sembach, K.R. 1991, *ApJ*, 379, 245
- Sembach, K. R., & Savage, B. D. 1992, *ApJS*, 83, 147
- Sembach, K. R., Savage, B. D., & Hurwitz, M. 1999, *ApJ*, 524, 98
- Sembach, K. R. et al. 2000, *ApJ*, this issue
- Sembach, K. R., Savage, B. D., & Tripp, T. M. 1997, *ApJ*, 480, 216
- Sahnow, D., et al. 2000, *ApJ*, this issue
- Shapiro, P.R., & Field, G. B. 1976, *ApJ*, 205, 762
- Shelton, R.L. 1998, *ApJ*, 504, 785
- Shelton, R. L., & Cox, D. P. 1994, *ApJ*, 434, 599
- Shull, J. M., & Slavin, J. D. 1994, *ApJ*, 427, 784
- Shull, J. M. et al., 2000, this issue (H2 paper)
- Slavin, J. D., Shull, J. M., & Begelman, M. C. 1993, *ApJ*, 407, 83
- Spitzer, L. 1956, *ApJ*, 124, 20
- Spitzer, L. 1990, *ARA&A*, 28, 71
- Spitzer L. 1996, *ApJ*, 458, L29

Sutherland, R. S., & Dopita, M. A. 1993, ApJS, 88, 253

Widmann, H., et al. 1999, A&A, 338, L1

York, D. G. 1977, ApJ, 213, 43



This preprint was prepared with the AAS L^AT_EX macros v5.0.

Fig. 1.— Portions of the FUSE spectra of PG 0804+761 and Ton S210 over the wavelength range from 1020–1045 Å. Galactic atomic absorption lines are identified. Galactic H₂ lines are indicated with the tick marks. The O VI λ1037.62 line lies near strong absorption by C II* λ1037.02 and the H₂ (5–0) R(1) and P(1) lines at 1037.15 and 1038.16 Å. The O VI 1031.93 Å line is usually relatively free of blending since the nearby H₂ (6–0) R(3) and R(4) lines at 1031.19 and 1032.36 Å are often weak. The day and nighttime integration for PG 0804+761 shows airglow emission from O I at the positions marked with the ⊕. Both integrations are contaminated by emission from terrestrial Lyβ λ1025.72.

Table 1. Results Based on the O VI $\lambda 1031.926$ Line

Object	V	z	l ($^{\circ}$)	b ($^{\circ}$)	T_{exp} (ksec)	$W_{\lambda} \pm \sigma$ (mÅ)	v_- (km s^{-1})	v_+	$\log N \pm \sigma$ (10^{14} cm^{-2})	$\log [N \sin b]$	h^a (kpc)
PG 0052+251	15.4	0.155	123.9	-37.4	16.8	<200 (3σ)	-150	+150	<14.20 ^b	<13.98	<1.6
PG 0804+761	15.2	0.100	138.3	+31.0	39.6	286 \pm 19	-160	+80	14.50 \pm 0.04	14.21	2.6
ESO 141-55	13.6	0.037	338.2	-26.7	35.8	256 \pm 21	-100	+100	14.50 \pm 0.05	14.15	2.3
VII Zw 118	14.6	...	151.4	+26.0	42.8	144 \pm 35	-100	+100	14.16 \pm 0.14	13.80	1.0
H 1821+643	14.2	0.297	94.0	+27.4	48.2	319 \pm 20	-175	+100	14.57 \pm 0.05 ^c	14.23	2.8
Mrk 509	13.1	0.034	36.0	-29.9	54.9	395 \pm 20	-95	+160	14.70 \pm 0.04 ^c	14.40	4.1
Mrk 876	15.5	0.129	98.3	+40.4	45.9	223 \pm 15	-100	+60	14.38 \pm 0.04 ^c	14.19	2.5
Ton S180	14.3	0.062	139.0	-85.1	16.6	240 \pm 22	-75	+120	14.43 \pm 0.06 ^c	14.43	4.3
Ton S210	15.2	0.117	225.0	-83.2	13.5	369 \pm 36	-130	+170	14.64 \pm 0.06 ^c	14.64	7.0
PKS 2155-304	13.1	0.116	17.7	-52.3	37.1	201 \pm 12	-70	+150	14.31 \pm 0.04 ^c	14.21	2.6
NGC 7469	...	0.016	83.1	-45.5	29.9	117 \pm 18	-100	+90	14.16 \pm 0.09 ^c	14.01	1.7
3C 273	12.8	0.158	290.0	+64.4	14.84 \pm 0.11 ^d	14.80	10.

^aThe value of this scale height assumes $n_0(\text{O VI}) = 2 \times 10^{-8} \text{ cm}^{-3}$.

^bLimit assumes a linear curve of growth.

^cThe column density and equivalent widths do not include contributions from high velocity gas detected beyond the listed integration range (v_- to v_+). This high velocity gas is discussed by Sembach et al. (2000).

^dThe value of $N(\text{O VI})$ for 3C 273 is an ORFEUS result from Hurwitz et al. (1998).